



APPLICATION OF NEW BOUNDING SURFACE PLASTICITY MODEL FOR CYCLIC LOADING OF SATURATED SANDS

M. Maleki¹, S. H. Hashemolhosseini² and A.M. Halabian³

¹ Grad. Student, Faculty of Civil Engineering, Isfahan University of Technology, Isfahan, Iran

² Associate Professor, Faculty of Mining, Isfahan University of Technology, Isfahan, Iran

³ Assistant Professor, Faculty of Civil Engineering, Isfahan University of Technology, Isfahan, Iran

Email: hamidh@cc.iut.ac.ir, mahdi@cc.iut.ac.ir

ABSTRACT :

Cyclic response of geomaterials is complex due to the pressure and specific volume dependency of the stress-strain relationship and the highly nonlinear behavior of the soil. This is particularly the case under undrained conditions in granular soils, where repeated loading and unloading can lead to a substantial rise in the pore water pressure and a sudden loss in the shear strength and the stiffness of the soil. Concerted efforts have been made to develop some plasticity models to predict non-linear behavior of soils. Conventional plasticity models such as Cam clay always assume a fixed shape of yield surface with a purely elastic interior domain, associative flow rule and using isotropic hardening rule for the evolution of the yield surface. These attributes lead to conceptually simple, non-rigorous and computationally efficient models. Cam clay model has some weakness, such as overestimating peak strength of over-consolidated clays and dense sands and unable to predict the static liquefaction failure observed in undrained loading of loose sands. Assumption of a purely elastic domain inside the yield surface limits the ability of these models to predict plastic deformations during unloading and subsequent reloading stages of a cyclic loading, which can lead to dynamic liquefaction in loose sand. This research is aimed to use bounding surface plasticity model to predict non-linear behavior of saturated soil subjected to dynamic loading. This method is computationally simple, uses fewer model parameters and results of the simulation fit experimental data with reasonable accuracy.

KEYWORDS: saturated sands, cyclic Loading, constitutive equation, bounding surface plasticity



1. INTRODUCTION

Soil modeling in geotechnical engineering has developed rapidly in the past recent years as a result of increasing need for more accurate prediction of material nonlinearity within computer codes. The efforts in developing new soil constitutive models are now concentrated on two more objectives. The models should be conceptually simple and computationally efficient to solve geomechanic problems. Behavior of soil-structure systems under cyclic loading such as earthquake and waves loading has been one of the main research areas in civil engineering for the past three decades. Accurate evaluation of the structural response in soil-structure systems as well as prediction of some geotechnical phenomena such as liquefaction could be strongly influenced by cyclic behavior of soil. Accordingly, any soil constitutive model used in the numerical models of geotechnical problems should be capable to assess the cyclic behavior of soil in the corresponding stresses state.

The conventional elasto-plastic models are based on the assumption of interior elastic domain of the yield surface in the stress space. This assumption causes conventional plasticity models to fail for predicting of plastic deformation during cyclic loading. To overcome this main problem, several cyclic plasticity models have been developed by modifying conventional theory of plasticity. The major development in cyclic constitutive elasto-plastic models has been based on the kinematic hardening theory (Mróz 1979, Lade 1997), generalized plasticity theory (Zienkiewicz 1985, Pastor 1990) and the bounding surface plasticity theory (Dafalias and Herrmann 1980, Bardet 1986, Manzari and Dafalias 1997, Dafalias and Manzari 2004).

Kinematic hardening models employ translation and/or rotation of the yield surface in the stresses space. However, these models require considerable computer memories to follow the history of sub-yield surfaces and the stress reversal surfaces as well. The models are not also appropriate in terms of time efficiency for numerical computations. Generalized plasticity theory, utilizes the unit normal to the yield surface and the plastic potential surface as well, instead of the explicit definition of both yield and potential surfaces in the stress space. Using separate hardening for loading and unloading stress paths, also incapability to satisfy consistency condition are the main setbacks for these models.

On the other hand, bounding surface plasticity models are based on this fact that plastic deformations occur even when the stress state lies inside the yield surface. These models use the conventional plastic flow rule, where the plastic strain increment is computed at an image stress point on the bounding surface. Employing an appropriate projection rule relates this image stress point to the actual stress point on the current loading surface. Bounding surface models are conceptually simple, while using less material constants; they showed good capability to predict different cyclic and monotonic loading paths with the experimental data (Habte (2006)). One of the most popular and efficient bounding surface models which is recently developed, is a model developed by Manzari and Dafalias (1997), and Dafalias and Manzari (2004). In the present study this model has been examined more precisely and is tried to overcome its drawbacks and also to simplify it.

2. SIMPLE BOUNDING SURFACE PLASTICITY MODEL FOR SANDS

Dafalias and Manzari (2004) proposed a comprehensive constitutive model for sands based on two main concepts: 1) the concept of yield/bounding or two surface plasticity formulation; and 2) the state parameter concept. State parameter is difference between current and critical void ratio at the same mean effective stress. According to this parameter, loose sands with positive state parameter, have contractive behavior and dense sands with negative state parameter show dilatancy behavior.

$$\psi = e - e_c \quad (2.1)$$

The formulation is consistent with the critical state framework. It is assumed that only change in the stress ratio ($\eta = q/p'$) can cause plastic deformation. The basic parameters of the model are defined in the triaxial stress space, q and p' . The incremental elastic and plastic stress-strain relations can be written as

$$d\varepsilon_q^e = dq/3G, \quad d\varepsilon_v^e = dp'/K \quad (2.2)$$

$$d\varepsilon_q^p = d\eta/H, \quad d\varepsilon_v^p = d \left| d\varepsilon_q^p \right| \quad (2.3)$$

in which ε_q^e and ε_v^e also ε_q^p and ε_v^p are volumetric and deviatoric elastic and plastic strains, respectively. Elastic response of the model is based on the hypoelastic model, which uses the tangent bulk, K , and tangent shear moduli, G . d and H are the dilation parameter and hardening plastic modulus corresponding to the increment of stress ratio, $d\eta$, respectively. As the model uses deviatoric plasticity, the yield function is depending on the stress ratio given by:

$$f = |\eta - \alpha| - m = 0 \quad (2.4)$$

In which α is the back stress ratio, which determines the center of the yield surface in the deviatoric plane and m is the radius of the wedge type yield surface. Figure 1 shows yield, critical, dilatancy, and the bounding surfaces of the model in p' - q space.

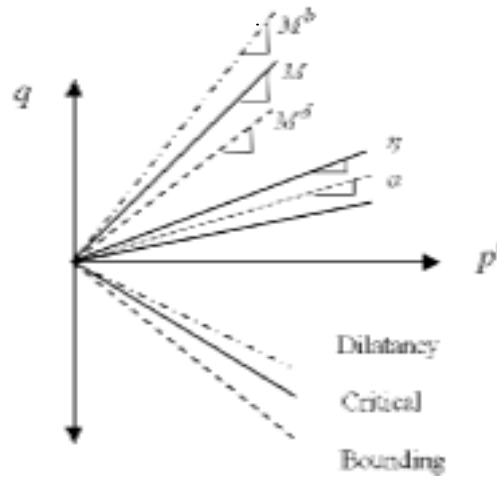


Figure 1. Schematic presentation of yield, critical, dilatancy and bounding surface

In Figure 1, the bounding stress ratio M^b , and dilatancy stress ratio M^d , are related to the state parameter and the critical stress ratio, M , as:

$$M^b = M \exp(-n^b \psi) \quad (2.5)$$

$$M^d = M \exp(n^d \psi) \quad (2.6)$$

In the above equations, n^b and n^d are positive material constants. From these equations it can be easily deduced that: for loose sands with contractive behavior $\psi > 0$, $M^d < M < M^b$; while for dense sands with $\psi < 0$, $M^b < M < M^d$ and at the critical state where $\psi = 0$, $M^d = M = M^b$. According to the critical state notion there will be no volume change at this stage. Here the hardening, softening and failure behavior occur at $H > 0$ for $\eta < M^b$, $H < 0$ for $\eta > M^b$ and $H = 0$ for $\eta = M^b$, respectively.

2.1. Plastic modulus

In this model, plastic modulus is function of the distance between current and bounding stress ratio as:

$$H = h(M^b - \eta) \quad (2.7)$$

where h is a scalar function which measures the distance between current and bounding stress ratio. $h = (M^b - \eta)$.



and is given by:

$$h = b_0 / (\eta - \eta_{in}) \quad (2.8)$$

η_{in} is the stress ratio at beginning of the loading process and is updated at any loading reversal. b_0 is a parameter depending on the p' and e .

2.2. Stress-dilatancy

Another basic equation of any elasto-plastic critical state model is the stress-dilatancy relation. In this model, Rowe's dilatancy theory is used as the form of following equation:

$$d = A_d (M^d - \eta) \quad (2.9)$$

in which A_d is also defined as the model parameter.

2.3. Critical state

The critical state is a state in which the combination of p' , q , e , satisfies simultaneously the critical state line (CSL). At this state, the stress ratio reaches to the critical stress ratio, $q_c / p'_c = M$, and the rate of volume change also is independent of the mean effective stress. Although the linear relation is conventionally used for relating $\ln(p')$ to e_c , for the sands the power law type relation could be more realistic as it is used in this model

$$e_c = e_0 - \lambda_c (p' / p_{at})^{\xi} \quad (2.10)$$

2.4. Fabric-dilatancy effect

For loose sands, continuous cyclic loading for the undrained conditions causes progressive build up to the pore water pressure resulting reduction of mean effective stresses. This fact is the most important reason of catastrophic events such as liquefaction and large permanent displacement in soil-structure system. To simulate this phenomenon, a key point so called the fabric change effect must be considered in the constitutive equation. Considering Eqs. (2.2) and (2.3), the undrained stress path, $d\varepsilon_v = d\varepsilon_v^e + d\varepsilon_v^p = 0$ leads to a relation between dilatancy parameter and the increment of mean effective stress, as $d\eta = 1/p'(dq - \eta dp')$. To reach a desirable result with progressive reduction in mean effective stress, the dilatancy parameter must be updated during the dilatancy phase of deformation. The observations made by Nemat-Naser and Tobita (1982) revealed that the great change in the particle contact-normal orientation during the dilation phase of deformation. By updating A_d with volumetric strain as:

$$A_d = A_0 (1 + \langle sz \rangle) \quad (2.11)$$

The desirable result may be obtained where the incremental relation for z is given by:

$$dz = -c_z \left\langle -d\varepsilon_v^p \right\rangle (sz_{max} + z) \quad (2.12)$$

in which z_{max} , is the maximum value of z , c_z is a constant parameter, and $\langle \rangle$ is the operator. According to MacCauly definition: $\langle x \rangle = \langle \rangle$ if $x > 0$, and $\langle x \rangle = 0$ if $x < 0$. Thus for dilation phase of deformation, with negative volumetric strain, dz is updated resulting an increase to the value of A_d , while for contractive deformation A_d will be constant. Larger value of A_d causes more reduction to the effective stress.



3. MULTIAXIAL GENERALIZATION

The wedge type yield surface in the triaxial stress condition is generalized to the cone type in the multiaxial stress space as

$$f = [(\mathbf{s} - p\mathbf{a}) : (\mathbf{s} - p\mathbf{a})]^{1/2} - \sqrt{2/3}mp' = 0 \quad (3.1)$$

where \mathbf{s} and \mathbf{a} are the deviatoric stress and the back stress ratio tensors. M , M^d and M^b can also be generalized to the corresponding critical, dilatancy, and bounding surfaces, respectively. Derivations of the yield function with respect to the stress tensor leads to the following equation:

$$\frac{\partial f}{\partial \boldsymbol{\sigma}} = \mathbf{n} - \frac{1}{3}(\mathbf{n} : \mathbf{r})\mathbf{I}; \quad \mathbf{n} = \frac{\mathbf{r} - \mathbf{a}}{\sqrt{2/3}m} \quad (3.2)$$

\mathbf{n} is the deviatoric component of the unit normal to the yield surface, \mathbf{r} is generalization of η from triaxial to the multiaxial stress space and \mathbf{I} is an identity vector. Using \mathbf{n} , Lode angle can be defined according to:

$$\cos(3\theta) = \sqrt{6}tr\mathbf{n}^3 \quad (3.3)$$

θ is varying from 0 to $\pi/3$, as the loading changes from compression to extension. Dafalias and Manzari (2004) used the following equation as the plastic potential surface:

$$g(\theta, c) = \frac{2c}{(1+c) - (1-c)\cos(3\theta)} \quad (3.4)$$

where c is the ratio of M in extension to the corresponding value in compression. Now, the variation of the back stress ratio which is used for kinematic hardening can be expressed as:

$$\boldsymbol{\alpha}_\theta^a = \sqrt{2/3} \alpha_\theta^a \mathbf{n}; \quad \alpha_\theta^a = g(\theta, c) \text{Exp}(\mp n^a \psi) - m \quad (3.5)$$

The index a in Equation (3.5) represents b , c , d for bounding, critical, and dilatancy surface respectively. Using non-associated flow rule the increments of plastic strains are obtained as:

$$d\boldsymbol{\varepsilon}^p = \langle L \rangle \mathbf{R}; \quad \mathbf{R} = \mathbf{R}' + \frac{1}{3}D\mathbf{I} = B\mathbf{n} - C\left(\mathbf{n}^2 - \frac{1}{3}\mathbf{I}\right) + \frac{1}{3}D\mathbf{I} \quad (3.6)$$

\mathbf{R}' is the deviatoric component of \mathbf{R} and D is the dilatancy parameter and

$$B = 1 + \frac{3}{2} \frac{1-c}{c} g \cos(3\theta); \quad C = 3\sqrt{3/2} \frac{1-c}{c} g \quad (3.7)$$

Based on the principle of the bounding surface theory and consistency condition, the loading index may be written as:

$$L = \frac{1}{K_p} \frac{\partial f}{\partial \boldsymbol{\sigma}} : d\boldsymbol{\sigma} = \frac{2G\mathbf{n} : d\boldsymbol{\varepsilon} - K\mathbf{n} : \mathbf{r} d\varepsilon_v}{K_p + 2G(B - tr\mathbf{n}^3) - KD\mathbf{n} : \mathbf{r}} \quad (3.8)$$

Now, the generalized form of the plastic modulus, dilatancy relation and fabric change is given as following equations:

$$K_p = (2/3)ph(\boldsymbol{\alpha}_\theta^b - \mathbf{a}) : \mathbf{n} = (2/3)ph \mathbf{b} : \mathbf{n}, \quad h = b_0 / ((\mathbf{a} - \mathbf{a}_{in}) : \mathbf{n}) \quad (3.10)$$

$$D = A_d(\boldsymbol{\alpha}_\theta^d - \mathbf{a}) : \mathbf{n} = A_d \mathbf{d} : \mathbf{n} \quad (3.11)$$

$$d\mathbf{z} = -c \left\langle -d\varepsilon_v^p \right\rangle (z_{max}\mathbf{n} + \mathbf{z}), \quad A_d = A_0 (1 + \langle \mathbf{z} : \mathbf{n} \rangle) \quad (3.12)$$

More details of these relations can be found in Manzari and Dafalias (1997), and Dafalias and Manzari (2004).

4. PROPOSED MODIFIED MOEDL

The major drawback associated with Dafalias and Manzari (2004) is related to the non-convexity of function $g(\theta, c)$, which is used for consideration of Lode angle effect in the bounding, critical, and dilatancy surfaces. Figure 2 shows

this non-convexity clearly. The lack of convexity becomes more serious for the soils with the friction angle exceeds 30° and consequently may cause negative plastic work and violation of thermo-mechanical principal laws. To overcome this problem, the function $g(\theta, c)$ used by Dafalias and Manzari (2004), Equation 3.4, is replaced by the surface proposed by Sloan, (Sheng *et. al* (2000)):

$$g_{mod}(\theta, c) = \left(\frac{2c^4}{(1+c^4) - (1-c^4)\sin(3\theta)} \right)^{0.25} \quad (3.4)$$

In this surface, the Lode angle is defined by following equation and varies between $-\pi/6$ to $\pi/6$ from extension to compression

$$\sin(3\theta) = \sqrt{6} \text{tr} \mathbf{n}^3 \quad (3.4)$$

This surface is convex for wide range of friction angles $0^\circ \leq \varphi'_{cs} \leq 48.50^\circ$.

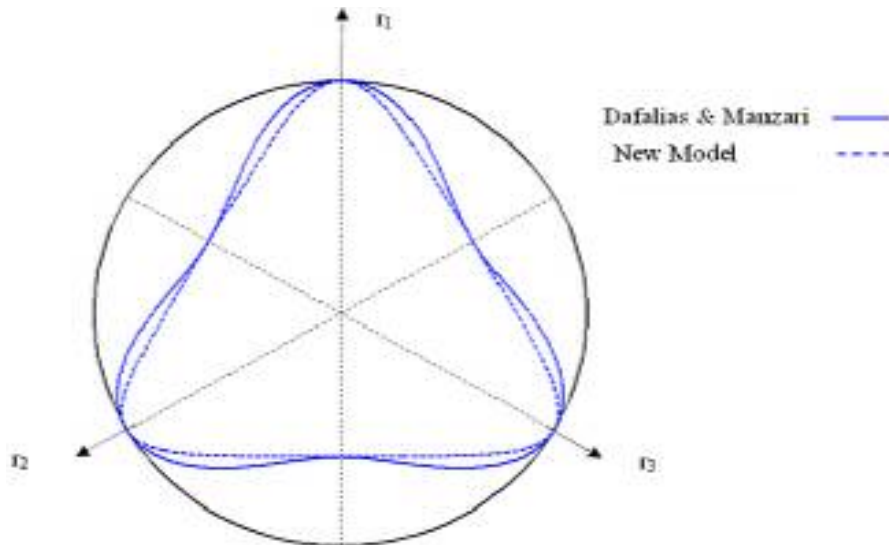


Figure 2 Comparison between Dafalias and Manzari (2004) and proposed models

5. RESULTS AND DISCUSSION

The proposed method in this study is employed to simulate the soil behavior of an undrained triaxial test under monotonic loading and a loose sand in a drained cyclic loading. Material constants used in these simulations are shown in Table 1.

Table 1 Model constants

Elastic parameters	G_0	125
	ν	0.05
Critical state	M_c	1.25
	c	0.712
	λ	0.019
	e_c	0.934
	ξ	0.74
Yield surface	m	0.01
Plastic modulus	h_0	7.05
	n^b	1.10
	c_h	0.968
Dilatancy	A_0	0.704
	n^d	3.50
Fabric-dilatancy tensor	Z_{max}	4
	c_z	600

5.1. Monotonic Loading

In the Figures (3a) and (3b) the results obtained for an undrained triaxial test are shown. Static liquefaction as one of important characteristics of loose sands behavior is simulated successfully. Experimental data given by Verdugo and Ishihara (1996) was used to verify the results. Figures (4a) and (4b) also show the good agreement between the results for the undrained behavior of dense sands (dilatancy behavior) and the experimental data.

5.2. Cyclic Loading

Figures (5a) and (5b) present the hysteretic stress-strain loops and volume changes for loose sands, in a drained loading test, respectively. Figure (6a) and (6b) also present the hysteretic stress-strain loops and volume changes for loose sands, in a drained loading test, respectively. It can be noted from Figures that the proposed model precisely simulated the soil behavior. The results from simulation of two undrained cyclic loading tests for loose and dense sands are shown in the Figure 7a. The hysteretic stress-strain loops for loose sands in the undrained cyclic loading test are also shown in Figure (7b). These Figures demonstrate that the capability of the proposed model to simulate dynamics liquefaction phenomenon.

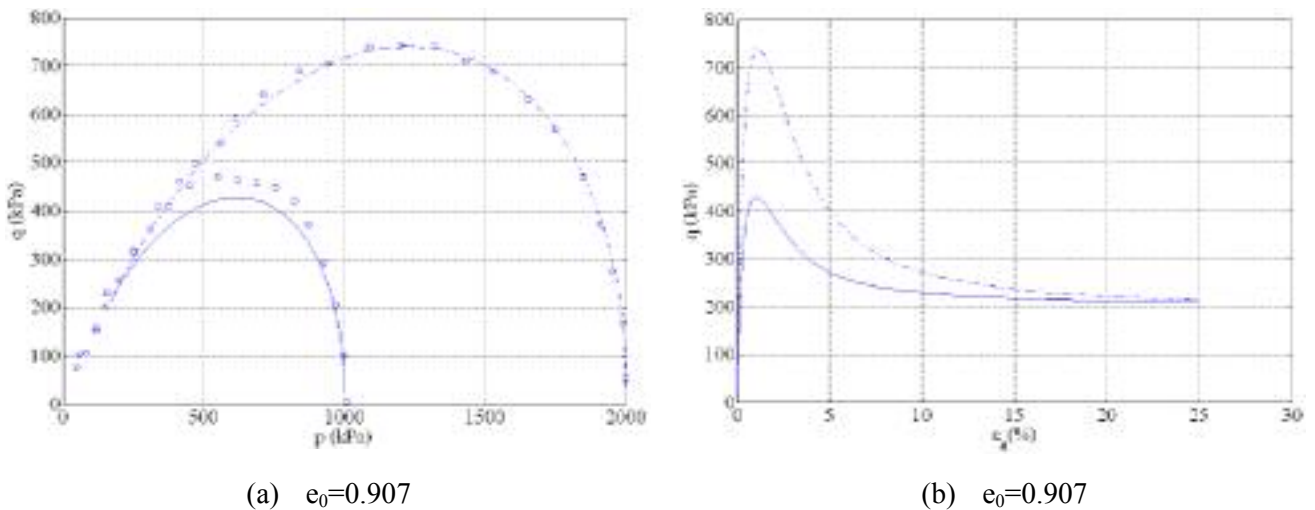
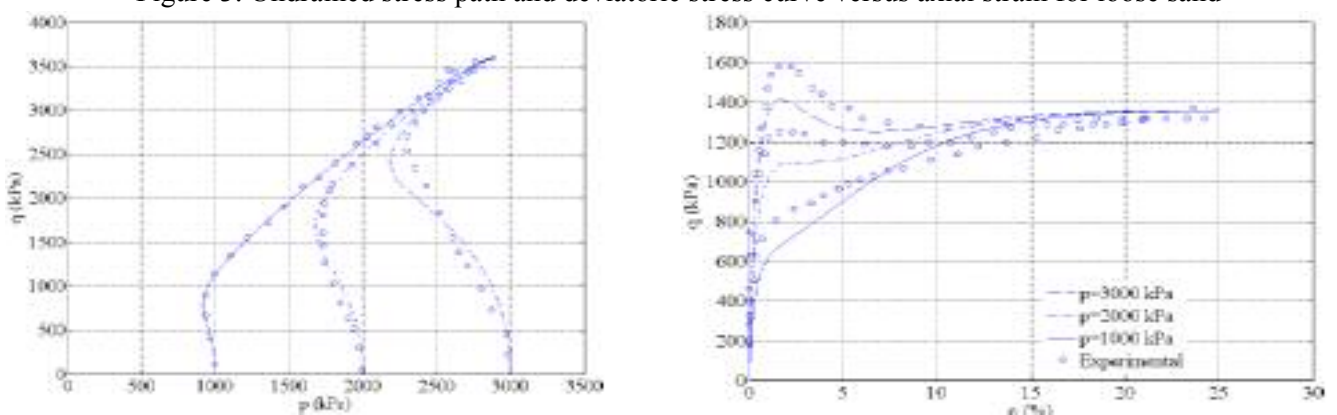
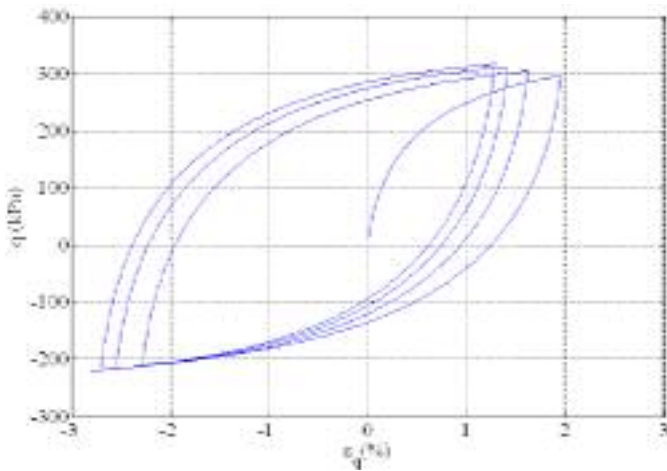
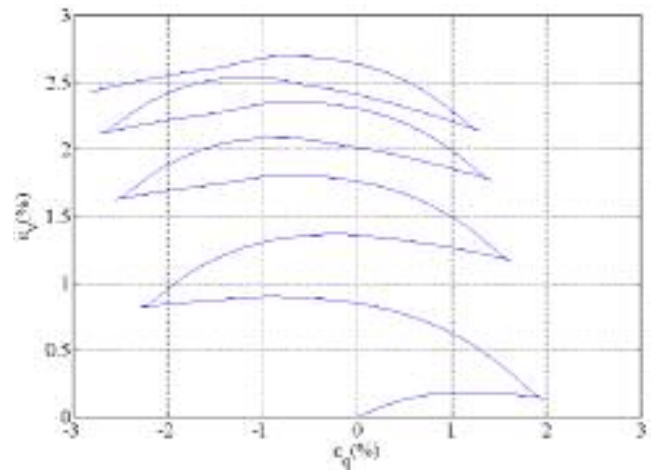


Figure 3. Undrained stress path and deviatoric stress curve versus axial strain for loose sand



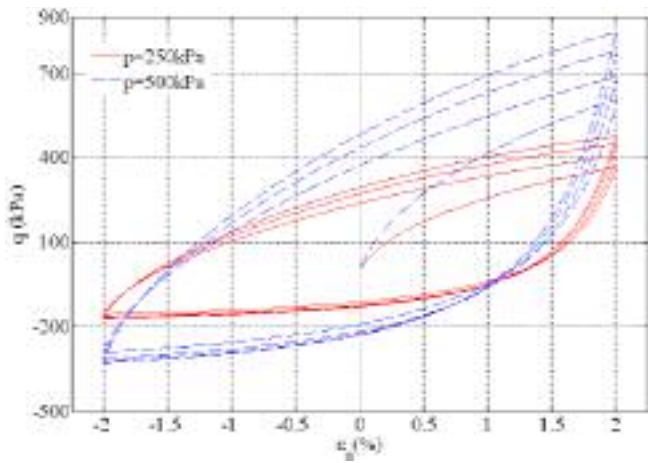


(a) $e_0=0.85$

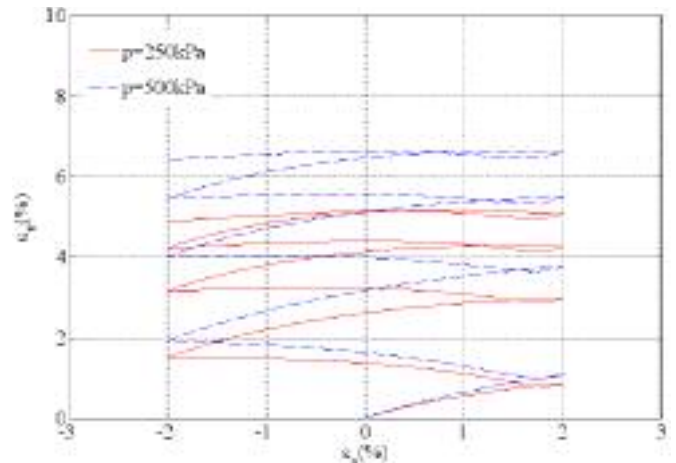


(b) $e_0=0.85$

Figure 5. Hysteretic loops and volume changes for a drained cyclic loading test on loose sand

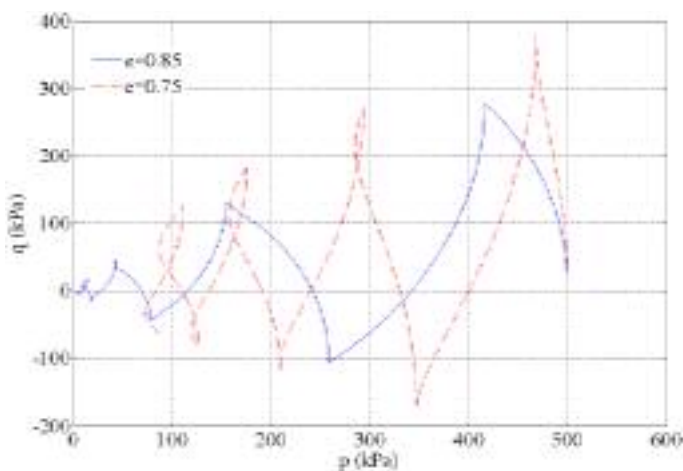


(a)

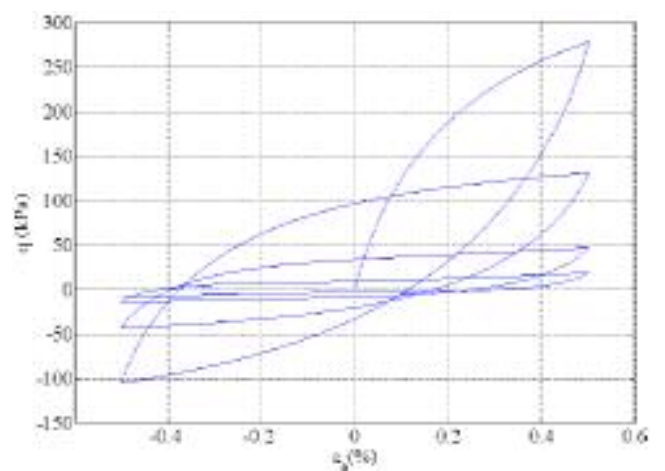


(b)

Figure 6. Hysteretic loops and volume changes for drained cyclic loading on a dense sand at two different confining pressure



(a)



(b) $e=0.85$

Figure 7. Undrained stress path for two different densities and hysteretic loops for loose sand in an undrained cyclic loading test (dynamic liquefaction)



6. CONCLUSIONS

Although Dafalias and Manzari (2004) model is capable to predict various type of loading paths, but its application may be restricted for some type of soils when $\phi'_{cs} \leq 30^\circ$, due to losing the convexity of the critical surface. In this paper, employing an alternative plastic potential surface, $g(\theta)$, the non-convexity problem of the model was solved and the model application range was extended to $\phi'_{cs} \leq 48.5^\circ$, which nearly covers all types of conventional geomaterials. The results obtained by this modified model both for monotonic and cyclic loading paths for loose and dense sands were shown to be quiet encouraging.

REFERENCES

- Chen, W. F. (1994). Constitutive equations for engineering materials. Vol 2. Plasticity and modeling. Elsevier, USA.
- Dafalias, Y. F., and Manzari, M. T. (2004). Simple plasticity sand model accounting for fabric change effects. *Journal of Engineering Mechanics* **130**: 6, 622-634.
- Habte, M. A. (2006). Numerical and constitutive modeling of monotonic and cyclic loading in variably saturated soils. *PhD Thesis of School of Civil and Environmental Engineering*, University of New South Wales, Sydney, Australia.
- Manzari, M.T., and Dafalias, Y. F. (1997). A critical two-surface plasticity model for sands. *Géotechnique***47**:2, 255-272.
- Nemat-Nasser, S. and Tobita, Y. (1982). Influence of fabric change on liquefaction and densification potential of cohesionless sand. *Mech. Mater.* **1**, 43-62.
- Sheng, D., Sloan, S. W., and Yu, H. S. (2000). Aspects of finite element implementation of critical state models. *Computational Mechanics* **26**:2,185-196.
- Verdugo, R., and Ishihara, K. (1996). The steady state of sandy soils. *Soils Found.***36**:2, 81-92.